Supporting information

Organogel electrolyte for high-loading silicon batteries

Yoon-Gyo Cho, Hyungmin Park, Jung-In Lee, Chihyun Hwang, Yuju Jeon, Soojin Park and Hyun-Kon Song*

Experimental

Cell preparation. 2032 coin-type half-cells (CR2032) were assembled with a carbon-coated silicon-based composite electrode as an anode and lithium metal as a counterpart. Porous polyethylene separator (NH716, Asahi) was used. Anode slurries were prepared by mixing silicon particles, a conducting agent and a mixed polymer binder at the wt. % compositions of 80:10:10 and 60:20:20 (for silicon nanoparticle) and 70:10:20 (for silicon microparticles). Nanoparticles of 100 nm size or micro-particles of 10 um size (Alfa Aesar) were used as the silicon active materials while carbon black (Super-P, TIMCAL) was used as the conducting agent. The mixed binder composed PAA and CMC in 50 to 50 wt. % (PAA = poly(acrylic acid) with weight average molecular weight = 100 kg mol^{-1} from Sigma Aldrich; CMC = sodium carboxymethyl cellulose with 4 wt. % in H_2O from Sigma Aldrich). A planetary centrifugal mixer (ARE-310, Thinky) was used for the mixing at 2,000 rpm with zirconia balls in the presence of a dose of water as a dispersion solvent for 5 min. The slurries were coated onto copper foils, followed by drying at 150 ^{o}C under vacuum for 2 h. Silicon loadings of electrodes (L_{Si}) were calculated in mg_{Si} cm^{-2} from the silicon masses used in half coin cells and the apparent electrode area (1.54 cm^2 from diameter = 7 mm).

Electrolytes. Used as liquid electrolyte was 1.3 M $LiPF_6$ in a mixture of ethylene carbonate (EC) and diethyl carbonate (DEC) (30:70 v/o) with 5 or 10 wt. % fluoroethylene carbonate (FEC). 2 wt. % of cyanoethyl polyvinyl alcohol (PVA-CN) polymer was dissolved in the base liquid electrolyte for GPE. All electrolytes were prepared in a glove box under controlled atmosphere with < 0.1 ppm oxygen and moisture. The cells containing the PVA-CN-present electrolyte were left for wetting for 12 h. Then they were charged and discharged at the currents equivalent to 0.05C based on the assumption of the capacity of silicon = 2000 mAh g^{-1} for solid-electrolyte interphase (SEI) layer formation at its pre-cycle. The currents of

the pre-cycles were 0.07 and 0.06 mA cm^{-2} for 80 and 60 wt. % 100 nm Si respectively and 0.10 mA cm^{-2} for 70 wt. % 10 um Si. After the pre-cycle, the cells were stored at 60 $^{\circ}$C for 12 h for *in situ* gelation (Fig. S1). The capacities at the pre-cycle (Q_{pre} in mAh cm^{-2}) were used as the available capacities of electrodes at the corresponding active mass densities.

Electrochemical characterization. Cells were galvanostatically charged and discharged in the potential window from 0.01 to 1.2 V (vs. Li/Li^{+}) by a battery tester (WonATech, WBCS 3000). Cyclic voltammograms were obtained by using a potentiostat (Biologic, VMP 3) at a scan rate of 0.1 mV s^{-1}. Electrochemical impedance spectra were obtained in a frequency range of 100 mHz to 1 MHz by the same potentiostat equipped with an impedance analyser.

Morphological and compositional characterization. Morphologies and compositions of carbon-coated silicon particles and electrodes were examined by a field emission scanning electron microscope (FE-SEM; Hitachi S-4800) and a high-resolution transmission electron microscope (HR-TEM; JEM-2100F) equipped with an energy-dispersive X-ray spectroscope (EDS) (Fig. S2). The X-ray photoelectron spectroscopy (XPS) analysis was performed with a K-alpha XPS (Thermo Fisher). Before analysing, all samples were washed in dimethyl carbonate (DMC) to clean and remove the electrolyte on the electrode particles in dry-room.

Table S1. Capacity comparison of selected high-loading silicon anodes.

Structure	Composition (A:B:C) [b]	L_{Si} [c] (mg$_{si}$ cm^{-2})	Q_{pre} [e] (mAh cm^{-2})	Q / Cyc / i [f] (mAh cm^{-2} / cycle / mA cm^{-2})	Ref
Si@C [a] (~100 nm)	80:10:10	1.3	3.3	2 / 150 / 0.66	1
	60:20:20	0.8	1.6	0.74 / 500 / 0.72	
Si@C [a] (~10 um)	70:20:10	1.6	3.4	2.3 / 50 / 0.7	
Si (800 nm)	-	1.1	3.2	2.7 / 120 / 0.3	2
Si@C [a] (pomegranate)	80[d]:10:10	3.1	~3.6	~3 / 100 / 0.7	3
nano-Si secondary cluster	65[d]:20:15	2.0	~3.5	~2.3 / 100 / 0.5	4
MSS@C [a] (800 nm)	A+C = 46 or 40 B = 20	0.5	~3	~1.5 / 300 / 0.75	5
Si microparticles	A = 50 B+C = 50	0.5 ~ 0.7	1.5-2.1	1,400 mAh g^{-1} / 120 / n.a.	6

[a] @C = carbon coating; MSS = mesoporous Si sponge. [b] A = active material (silicon here), B = binder, C= conducting agent. [c] L_{Si} = areal loading density of silicon. [d] carbon contents included in active materials. [e] Q_{pre} = delithiation capacity measured in the pre-cycle at 0.05C. [f] Q = capacity at the specified cycle (Cyc) in the specified current (i).

[1] This work. [2] Adv. Energy Mater. 2015, 1401826. [3] Nat. Nanotechnol., 2014, 9, 187. [4] Energy Environ. Sci., 2015, 8, 2371-2376. [5] Nat. Commun., 2014, 5, 4105. [6] Nat. Chem., 2013, 5, 1042-1048.
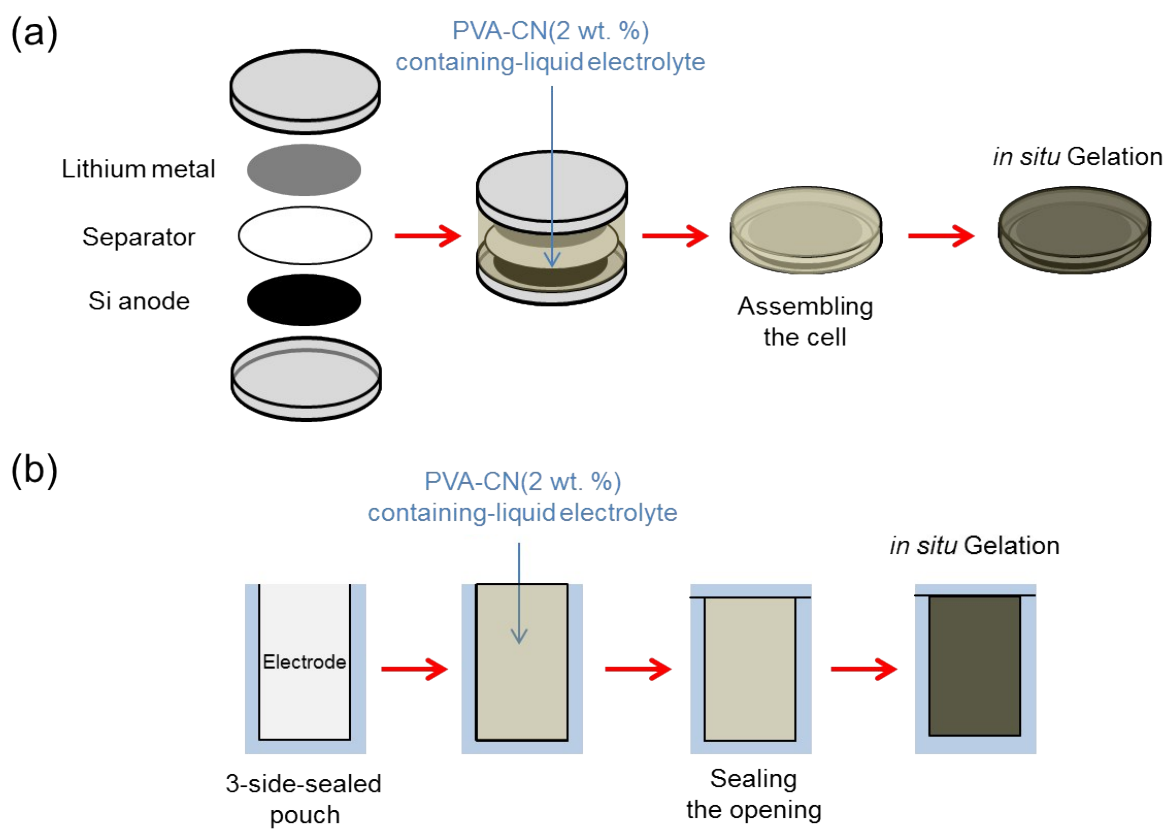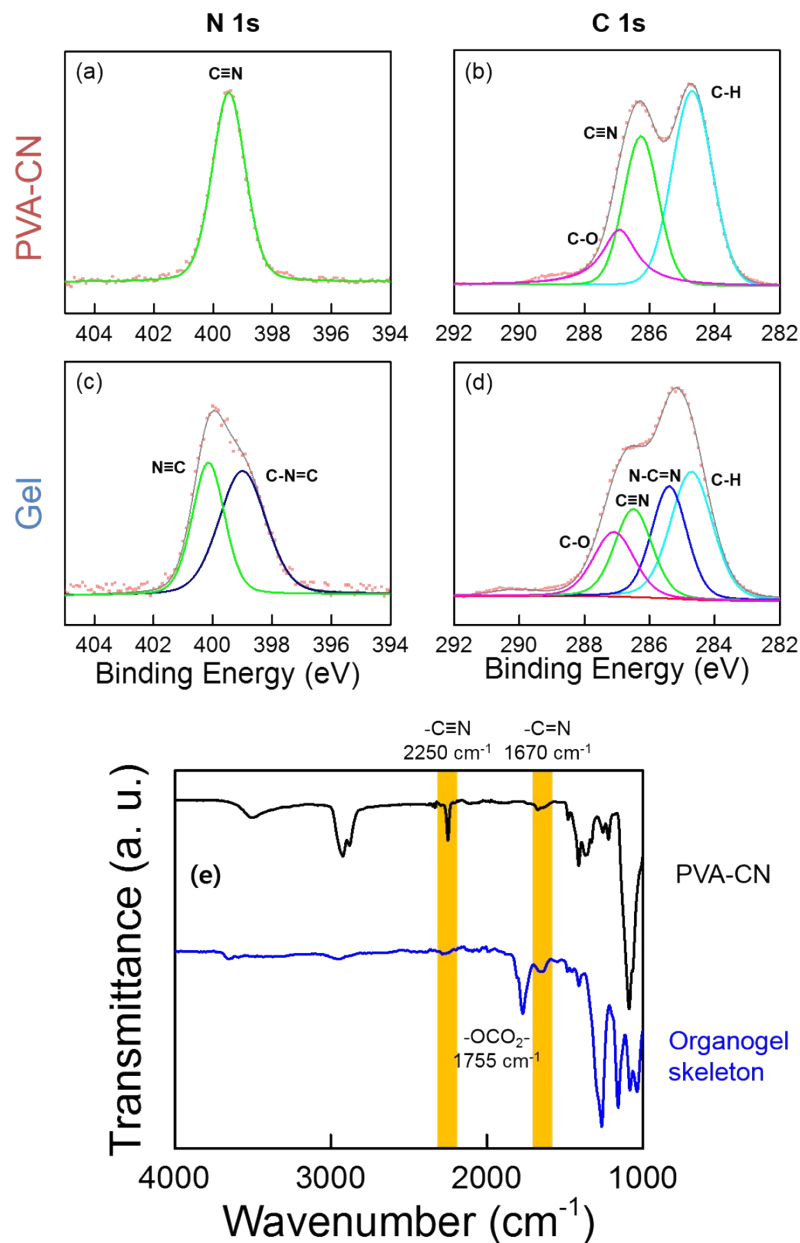
Fig. S1. *in situ* gelation of PVA-CN-containing liquid electrolyte within a coin cell (a) and a pouch cell (b).
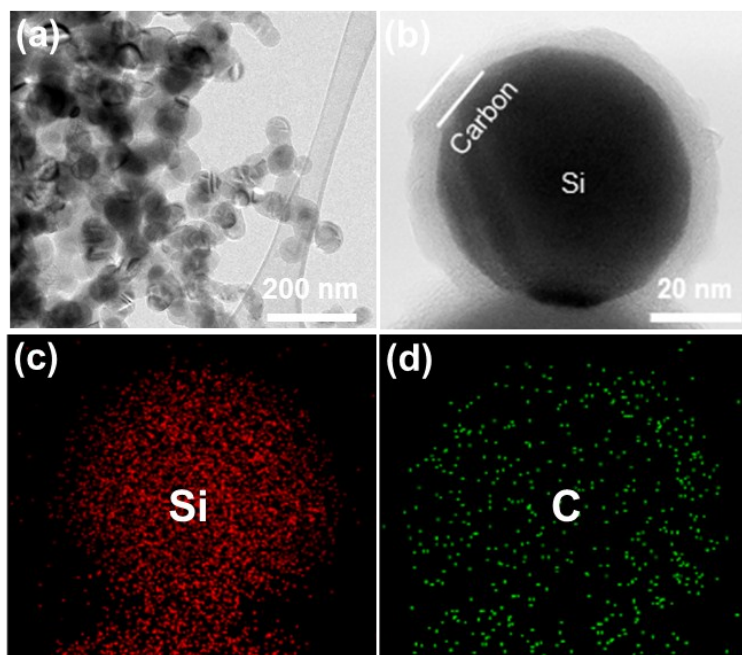
Fig. S2. Carbon-coated silicon nanoparticles used in this work. (a and b) TEM images. (c and d) Component maps of silicon and carbon by energy dispersive spectroscopy (EDS).
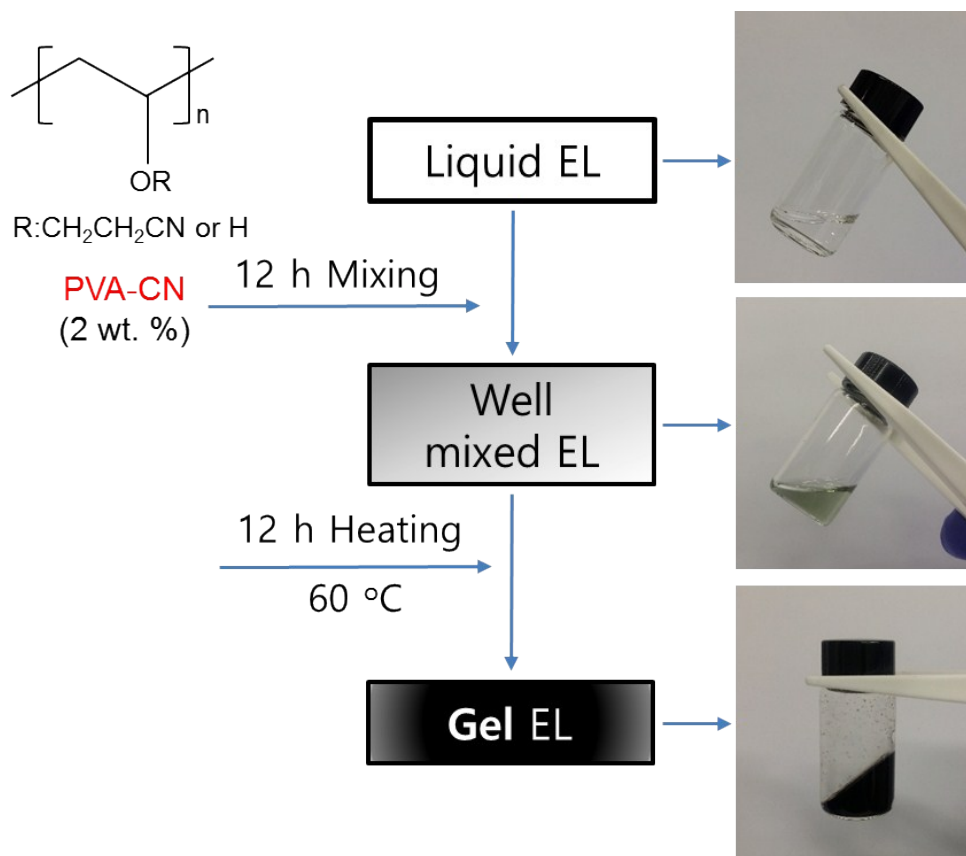
**Fig. S3.** Preparation of the gel electrolyte based on PVA-CN.

Fig. S4. Gelation confirmation. (**a** to **d**) X-ray photoelectron (XPS) N1s (a) and C1s spectra of PVA-CN (**a** and **b**) and gel electrolyte (**c** and **d**). (**e**) Fourier transform infrared (FTIR) spectra of PVA-CN and organogel skeleton. The organogel skeleton was obtained by drying the organogel electrolyte by a freeze dryer to remove the constituent liquid solvents. PVA-CN (before gelation) had a sharp peak at 2250 cm^{-1} belonging to C≡N with a broad and small peak at 1670 cm^{-1} for C=N. However, the intensity of the C≡N peak decreased significantly after gelation while C=N was observed obviously at 1670 cm^{-1}. The peak assigned to carbonate (CO_3^{2-}) at 1755 cm^{-1} is thought to come from carbonate solvents remaining after the drying process.
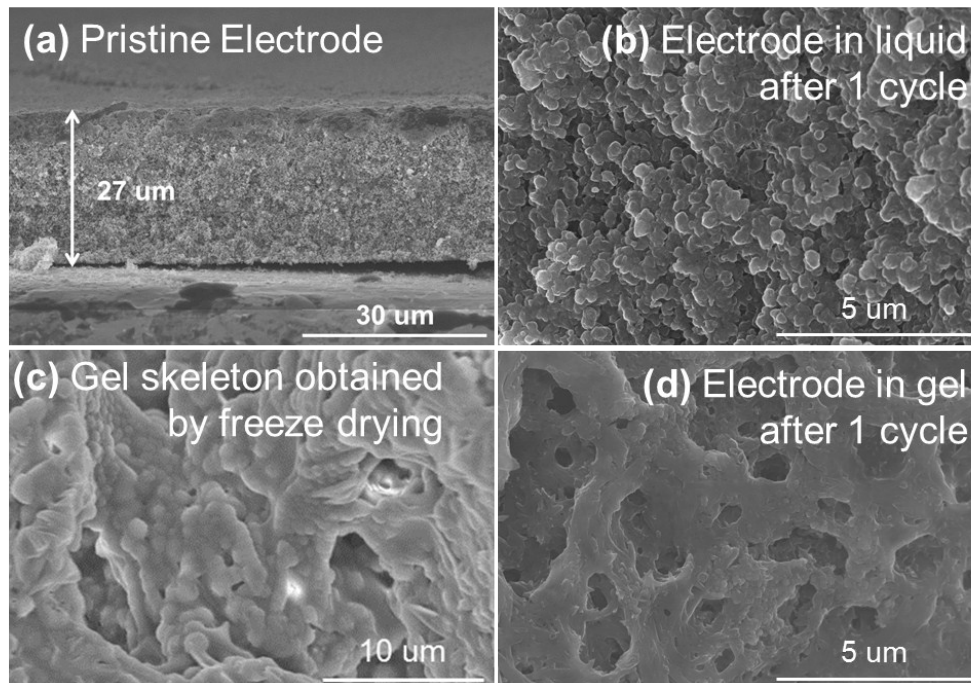
Fig. S5. SEM images of cross-sectional view of silicon electrodes (a, b, d) and gel skeleton (b). The gel network was visualized as a three-dimensional framework with high porosity.
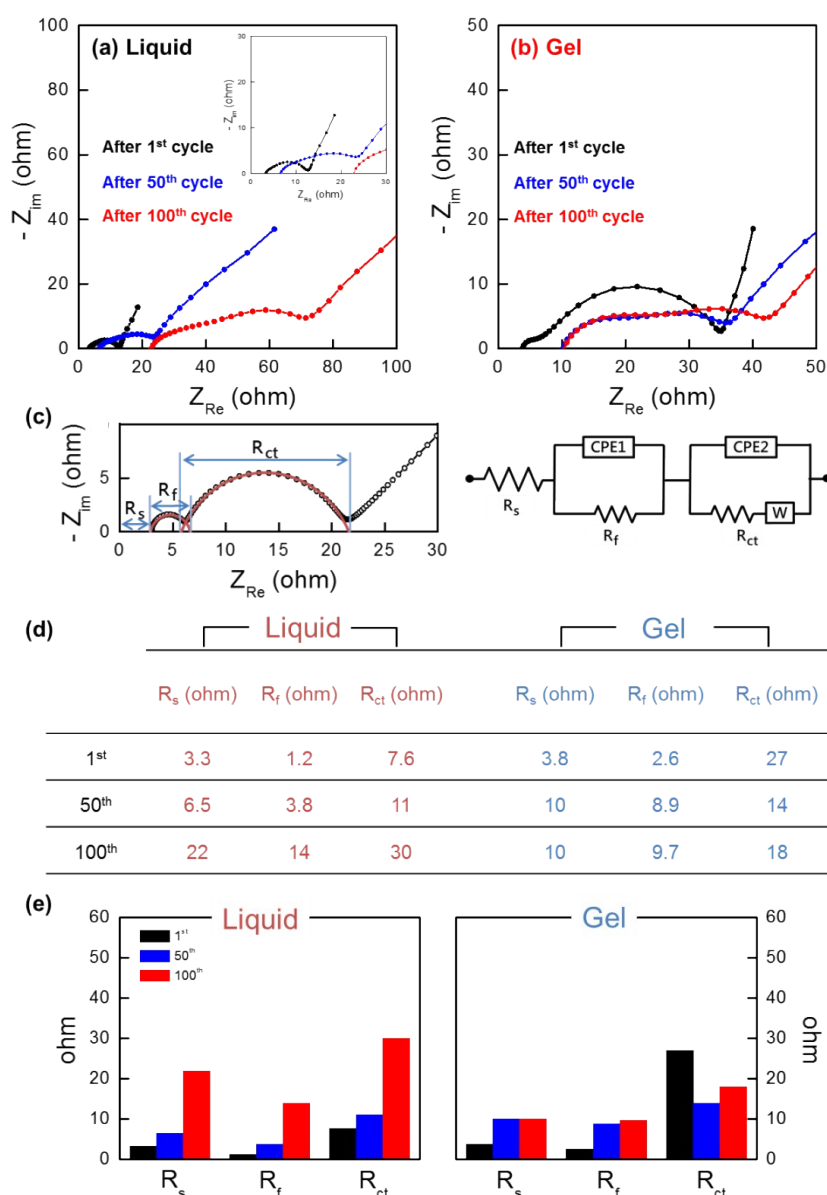
Fig. S6. Resistance components responsible for silicon lithiation kinetics traced along repeated cycles of lithiation and delithiation. (a and b) Impedance spectra obtained between 1 mHz to 1 MHz. (c) The equivalent circuit used for interpreting the spectra in a and b: R_s = solution resistance + contact resistance, R_f = surface film resistance, R_{ct} = charge transfer resistance; CPE1 = constant phase element representing capacitance on the interface between electrolyte and SEI layer, CPE2 = constant phase element representing capacitance on the interface between the SEI layer and silicon; W = Warburg impedance responsible for diffusion of lithium ions. (d and e) The component values of the equivalent circuit in b obtained by fitting the spectra in a and b.
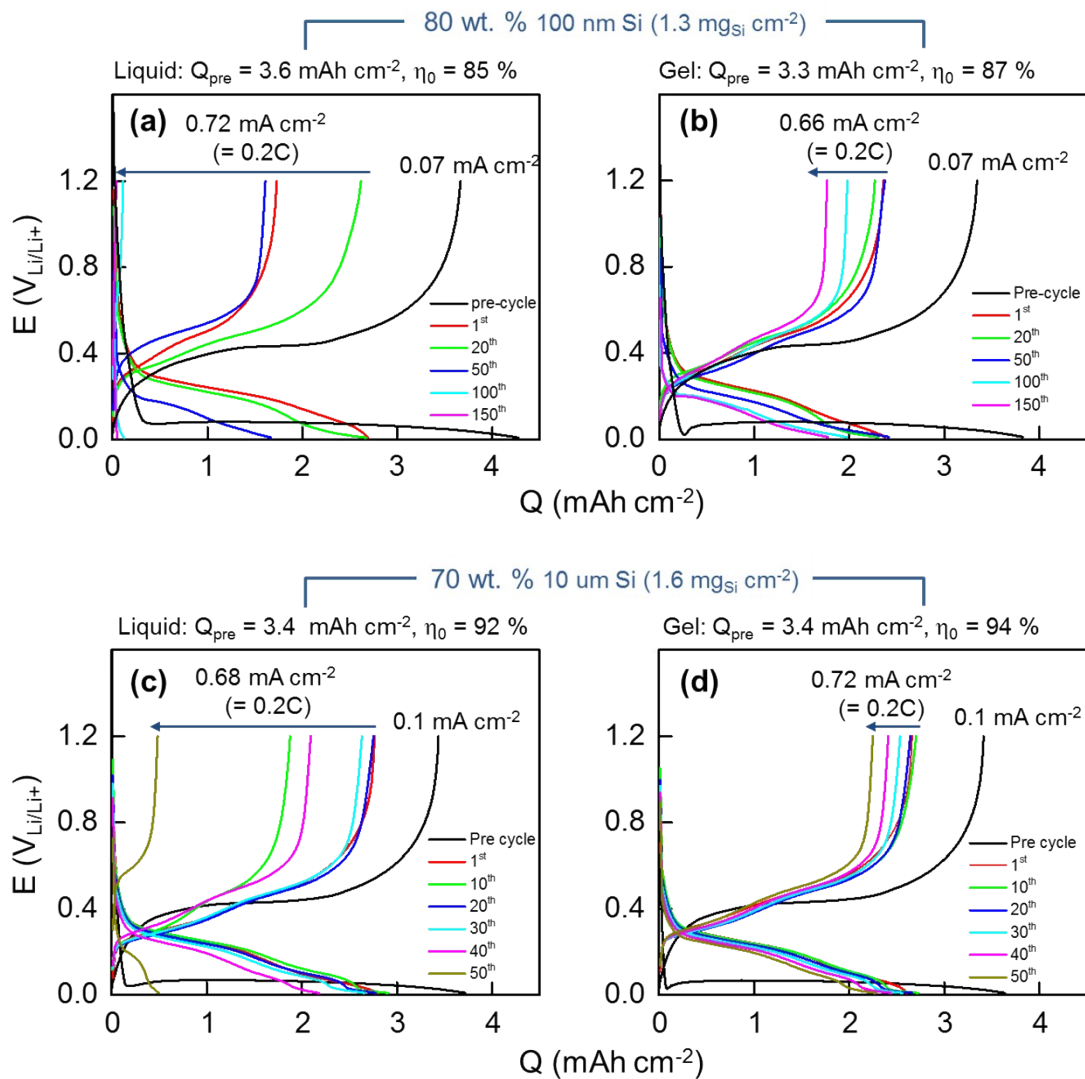
Fig. S7. Galvanostatic charge/discharge potential profiles (E = potential, Q = capacity). The initial pre-cycle was obtained at 0.1 mA cm^{-2} while other numbered cycles were obtained at specified current density. The capacities at the initial pre-cycle (Q_{pre}) and the initial coulombic efficiencies (η_0) were indicated. (a and b) Electrodes containing 80 wt. % 100 nm Si (1.3 mg$_{Si}$ cm^{-2}) in liquid (a) and gel (b) electrolytes. (c and d) Electrodes containing 70 wt. % 10 um Si (1.6 mg$_{Si}$ cm^{-2}) in liquid (c) and gel (d) electrolytes.
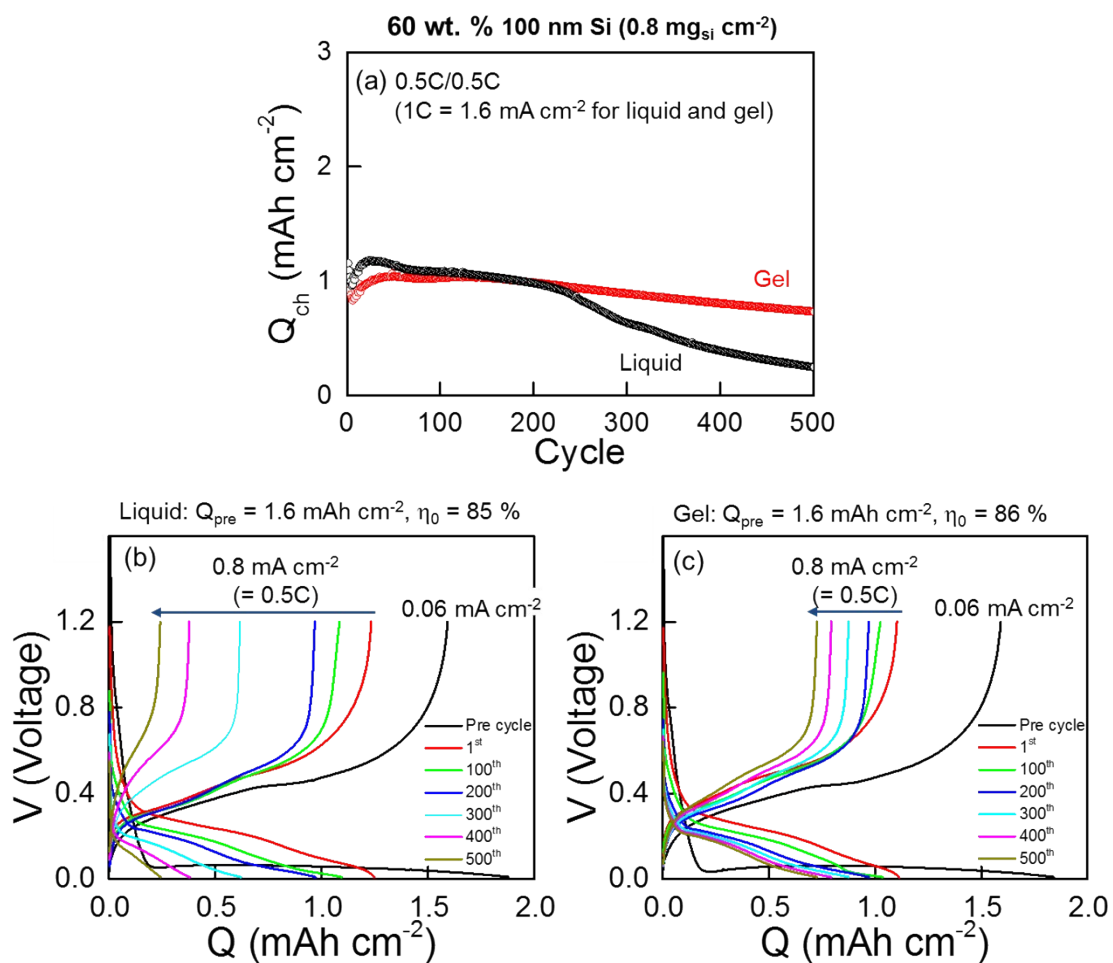
Fig. S8. Low-loading electrodes of 100 nm silicon nanoparticles (Lsi = 0.8 mg$_{Si}$ cm-2; X$_{Si}$ = 60 wt. %). (a) Capacity retention along cycles of 0.5C lithiation and 0.5C delithiation. (b and c) Potential profiles at selected cycles of a.